Mon. Not. R. Astron. Soc. **323**, 988–994 (2001)

# The effect of gas loss on the formation of bound stellar clusters

M. P. Geyer★ and A. Burkert
*Max-Planck-Institut für Astronomie, Königstuhl 17, D-69117 Heidelberg, Germany*

Accepted 2000 December 14. Received 2000 December 14; in original form 2000 July 31

**ABSTRACT**

The effect of gas ejection on the structure and binding energy of newly formed stellar clusters is investigated. The star formation efficiency (SFE), necessary for forming a gravitationally bound stellar cluster, is determined.

Two sets of numerical *N*-body simulations are presented. As a first simplified approach we treat the residual gas as an external potential. The gas expulsion is approximated by reducing the gas mass to zero on a given time-scale, which is treated as a free parameter. In a second set of simulations we use smoothed particle hydrodynamics (SPH) to follow the dynamics of the outflowing residual gas self-consistently. We investigate cases where gas outflow is induced by an outwards propagating shock front and where the whole gas cloud is heated homogeneously, leading to ejection.

If the stars are in virial equilibrium with the gaseous environment initially, bound clusters only form in regions where the local SFE is larger than 50 per cent or where the gas expulsion time-scale is long compared with the dynamical time-scale. A small initial velocity dispersion of the stars leads to a compaction of the cluster during the expulsion phase and reduces the SFE needed to form bound clusters to less than 10 per cent.

**Key words:** stars: formation – globular clusters: general – open clusters and associations: general.

## 1 INTRODUCTION

During the formation of star clusters gas expulsion, caused by feedback of young massive stars, terminates the star formation epoch and can unbind the stellar system. Many mechanisms leading to gas loss exist; for example, ionizing radiation, stellar winds or supernova explosions. It is still uncertain which of those play the major role.

The gas expulsion reduces the binding energy of the cluster. Hills (1980) showed, using analytic approximations, that a system of stars and gas losing more than half of its mass in less than a crossing time will disrupt. Thus, to obtain bound stellar clusters, a star formation efficiency (SFE) $\epsilon = M_{\rm s}/M_{\rm c} > 0.5$ is needed, where $M_{\rm s}$ and $M_{\rm c}$ are the mass of the stellar component and of the initial gas cloud prior to star formation, respectively. As the typical SFEs are less than 10 per cent, the formation of gravitationally bound old open clusters and globular clusters is an interesting and as yet unsolved problem.

Numerical simulations investigating the stability of young star clusters after gas expulsion have been performed by Lada, Margulis & Dearborn (1984). They showed that open star clusters, initially in virial equilibrium with the surrounding residual gas and containing up to 100 stars, can remain bound even if the SFE is as low as 30 per cent. In their simulations they treated the residual gas as a variable external potential added to that of the stars. Goodwin (1997) extended these simulations to globular clusters (GC), increasing the number of particles, allowing for different gas expulsion mechanisms and including loss of stars owing to the galactic tidal field. Klessen & Burkert (2000, 2001) presented high-resolution simulations of cluster formation in turbulent molecular clouds. Their models lead to bound clusters for very low SFEs. Additionally, a semi-analytic model by Adams (2000) also claims that the formation of bound star clusters occurs even for global SFEs much smaller than 50 per cent.

We present a new set of numerical simulations of the early evolution of young GCs, covering a broad range of SFEs and gas expulsion time-scales. Because the typical collision dominated relaxation time-scale of GCs is much larger than the dynamical time-scale, we restrict ourselves to collisionless *N*-body calculations for the stellar component. We present two sets of simulations. As a first assumption, in Section 2 we treat the residual gas as an external potential. We investigate the dynamics of the cluster during and after gas expulsion and derive constraints for the SFE required to form a bound cluster. Using a combined *N*-body and hydrodynamic code, in Section 3 we investigate the gas removal more self-consistently. Conclusions follow in Section 4.

★E-mail: geyer@mpia-hd.mpg.de

© 2001 RAS

## 2 GAS EXPULSION IN PURE *N*-BODY SIMULATIONS

Our simulations start after the cluster has formed, but before the residual gas has been expelled. The stars are represented by collisionless, equal mass *N*-body particles. The effect of the ejection of the residual gas on the stellar system is treated as a time variable external potential, similar to the approach of Lada et al. (1984).

In the following, all quantities are given in dimensionless code units (gravitational constant $G = 1$). Thus, taking typical globular cluster properties $\hat{M} = 10^5\,\mathrm{M}_\odot$ and $\hat{R} = 10\,\mathrm{pc}$ as mass and length units, respectively, we obtain a time unit $\hat{t} = (G\hat{\rho})^{-1/2} = 1.5 \times 10^6\,\mathrm{yr}$ (equal to the dynamical or crossing time-scale) with the density unit $\hat{\rho} = \hat{M}/\hat{R}^3$.

The *N*-body calculations are performed using a hierarchical tree method (Barnes & Hut 1986).

### 2.1 Initial configuration and the gas expulsion phase

To obtain a stable initial configuration, in a first step the stars are distributed according to a King (1966) distribution function with total mass equal to that of the initial gas cloud. The potential is tabulated and is used for modelling the external gas potential during the simulation. Therefore, stars and gas have equal density distributions. Finally, the mass of the stars and the gas are scaled according to the SFE. Now the stars are in virial equilibrium within the sum of their own potential and the potential of the gaseous component. The parameters of the different models are given in Table 1. For each model, the SFE is varied between 0.15 and 0.80.

To test whether the initial system is in virial equilibrium, several calculations without gas expulsion are performed. The density distributions are well conserved.

We simulate the gas expulsion starting at time $t = t_0$ by multiplying the external potential by a time-dependent factor

$$\xi = \begin{cases} 1 & \text{if} \quad t < t_0 \\ 1 - (t - t_0)/t_{\mathrm{exp}} & \text{if} \quad t_0 < t < t_0 + t_{\mathrm{exp}} \\ 0 & \text{if} \quad t > t_0 + t_{\mathrm{exp}}, \end{cases} \tag{1}$$

where $t_{\mathrm{exp}}$ is the time that is needed to drive the gas out of the system (gas expulsion time).

We can estimate the order of the gas expulsion time: the isothermal speed of sound of a molecular cloud gas with temperature $T = 10\,\mathrm{K}$ and molecular weight $\mu = 2.36$ is $a = \sqrt{R_{\mathrm{gas}} T/\mu} = 0.19\,\mathrm{km\,s^{-1}}$, where $R_{\mathrm{gas}}$ is the gas constant. If we consider a disruptive process that starts at the centre of a cloud as given by model N1 and travels outwards with speed of sound, it will need approximately a time of $t_{\mathrm{exp}} = R_{\mathrm{t}} a^{-1} \approx 6.6 \times 10^6\,\mathrm{yr}$ (or $t_{\mathrm{exp}} \approx 4$, given the dimensionless code units above) to reach the edge of the cloud. Fast processes (e.g. supernova explosions) may remove the gas on shorter time-scales. The gas expulsion time will therefore presumably be of the order of a dynamical time which is equal to the unit of time. In the simulations we use $t_{\mathrm{exp}} = 0$, 2, 4 and 10, which are equal to 0,7,14 and 36 crossing times at half-mass radius of model N1 and N3 and 0,12,24 and 59 crossing times of model N2.

**Table 1.** Parameters of the initial configurations (*N*-body). $W_0 = \psi(0)/\sigma^2$, scaled central potential of the King profile, see Binney & Tremaine (1987); $t_{\mathrm{c}}$, crossing time at half-mass radius; $R_{\mathrm{t}}$, tidal radius of King profile; $N$, number of particles used in simulation; $\delta$, numerical (Plummer) smoothing length; total mass (stars and gas) of all models was set to 1; all quantities are given in dimensionless code units (see text).

| Model | $W_0$ | $t_{\mathrm{c}}$ | $R_{\mathrm{t}}$ | $N$ | $\delta$ |
|---|---|---|---|---|---|
| N1 | 3.0 | 0.28 | 1.26 | 1000 | 0.1 |
| N2 | 5.1 | 0.17 | 1.33 | 1000 | 0.1 |
| N3 | 3.0 | 0.28 | 1.26 | 4000 | 0.05 |

### 2.2 Dynamics of the cluster during and after gas expulsion

The typical evolution of the *N*-body part of a cluster with $t_{\mathrm{exp}} = 2$ (seven crossing time-scales) is displayed in Fig. 1. Starting at $t = 20$ the external potential is slowly reduced to zero as described in the previous section. The cluster expands. A certain number of stars become unbound and start leaving the system. The bound ones relax after the gas has been completely removed, forming a broader configuration. A particle is believed to be unbound if its total energy (kinetic energy plus potential energy) is positive. This criterion is different from that of Goodwin (1997), who marked all stars outside a given tidal radius as unbound.

Fig. 2 shows the evolution of the Lagrangian radii containing 10 and 50 per cent of the *current bound* mass of the system and the virial ratio $\eta = -2E_{\mathrm{kin}}/E_{\mathrm{pot}}$ of the bound particles. The constant mass radii and virial ratios before gas expulsion show that initially the system is indeed in virial equilibrium. When the superimposed gas potential decreases ($t > 20$), the mass radii increase rapidly and relax for $t > t_{\mathrm{exp}}$. This behaviour is also reflected in the virial ratio. The system achieves a more extended equilibrium state.

The radial expansion factor of the cluster can be estimated as follows. In the adiabatic case (expulsion time-scale is much longer than the crossing time) $R \cdot M$ is constant and therefore (Hills 1980; Mathieu 1983) the ratio of final to initial radius is

$$\frac{R_{\mathrm{f}}}{R_{\mathrm{i}}} = \frac{M_{\mathrm{c}}}{M_{\mathrm{s}}} = \frac{1}{\epsilon} \qquad \text{with} \quad 0 < \epsilon \leq 1. \tag{2}$$

On the other hand, if the expulsion time is short compared with the crossing time, we can apply conservation of kinetic energy per particle during the ejection of the gas. Hills (1980) and Mathieu (1983) obtained

$$\frac{R_{\mathrm{f}}}{R_{\mathrm{i}}} = \frac{\epsilon}{2\epsilon - 1} \qquad \text{with} \quad \frac{1}{2} < \epsilon \leq 1. \tag{3}$$

If $\epsilon \leq 0.5$ the final system is unbound.

Fig. 3 shows the ratio of the final to the initial half-mass radii of the *bound* particles at the end of the simulations, compared with the theoretical predictions of equations (2) and (3). If stars are lost and the bound mass of the cluster is not conserved, equations (2) and (3) are no longer strictly valid and discrepancies with the analytic approximations occur.

As expected, the simulations with long gas expulsion time-scales fit well the full curve, representing the adiabatic case. The faster the gas expulsion, the larger is the ratio of the final to the initial radius compared with the theoretical result.

The models with fast gas expulsion follow the broken curve well for high SFEs. For low SFEs, the ratio of final to initial radii

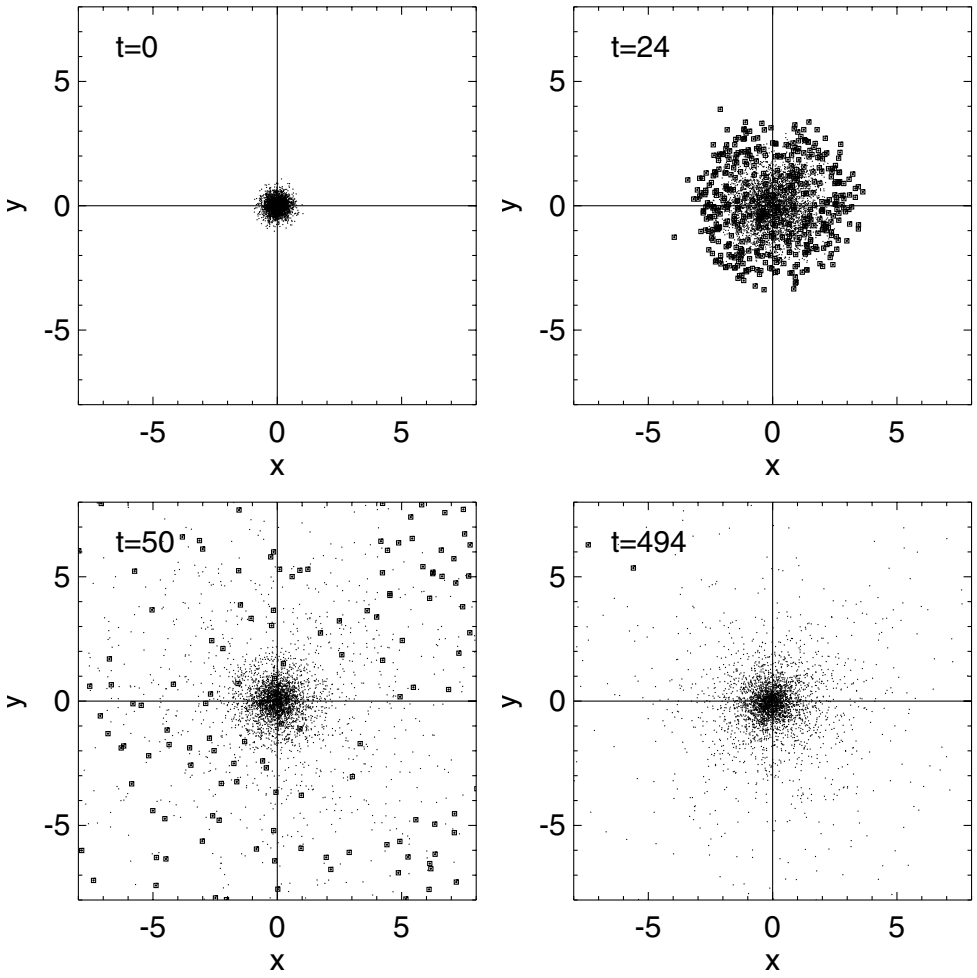


**Figure 1.** Time evolution of model N3. The time $t$ is given in dimensionless units. The SFE is $\epsilon = 0.4$, expulsion time $t_{\rm exp} = 2$. The plots show the $N$-body particles (small dots) projected on to the $x$–$y$-plane; unbound particles are indicated by squares.

is smaller than the analytical prediction, which emphasizes that the divergence for $\epsilon = 0.5$ does not occur in numerical simulations: the final radius is decreased by excluding the unbound particles which are located preferentially at high radii. Additionally, the outgoing particles reduce the total energy of the remaining system and leave behind a tighter bound core.

### 2.3 Constraints on the star formation efficiency

After the gas expulsion the system of the remaining bodies relaxes again (Fig. 2).

Fig. 4 shows the ratio of the number of finally bound stars to the initial number of stars for various SFEs and gas expulsion time-scales. The upper panel provides a resolution study of the runs N1 and N3 with 1000 and 4000 particles, respectively. Within the uncertainties they are indistinguishable. Large dots show results from Lada et al. (1984) obtained from simulations with 50 (!) stars. As can be seen, the number of particles used does not influence the results. This proves that the early results obtained by Lada et al. (1984) for open clusters also hold for GCs.

The lower panel compares the initially more concentrated King model (N2) to the less concentrated one (N1). We find that the curves of model N2 with $t_{\rm exp} > 0$ are shifted to lower star formation efficiencies or higher ratios of bound stars, respectively. This is caused by the lower half-mass crossing time of the more concentrated cluster N2 (Table 1), confirming that only the ratio of the expulsion time-scale to the crossing time is important. Thus, more concentrated clusters have a larger chance to survive. In the case of instantaneous gas expulsion ($t_{\rm exp} = 0$) the models N1 and N2 yield the same curve.

The ratio of bound to unbound stars gives a threshold for the SFE $\epsilon$ necessary to form bound clusters. In the case of instantaneous gas expulsion (see Fig. 4) the curves are centred around $\epsilon = 0.45$, which is somewhat less than the theoretical limit $\epsilon = 0.5$ for bound clusters given by Hills (1980).

Adams (2000) recently gave analytic approximations for the dependency of the number of bound stars on the SFE in the case of instantaneous gas expulsion. For a SFE $\epsilon = 0.5$ about 73 per cent of the stars are kept, in good agreement to our results from Fig. 4 ($t_{\rm exp} = 0$). However, our results show a stronger dependence of mass loss on the SFE $\epsilon$. In contrast to Adams (2000), star clusters with a SFE lower than $\epsilon = 0.4$ are dissolved in our simulations. This discrepancy can be understood from the fact that Adams uses density distributions of gas and stars with very different concentrations. Thus, even if the global SFE is small, the local SFE in the region of star formation could be as high as 90 per cent, leading to a bound system.

The number of finally bound stars increases with the gas expulsion time. In order for more than 50 per cent of all the stars to remain bound the SFE must be equal to 45, 30, 25 and 20 per

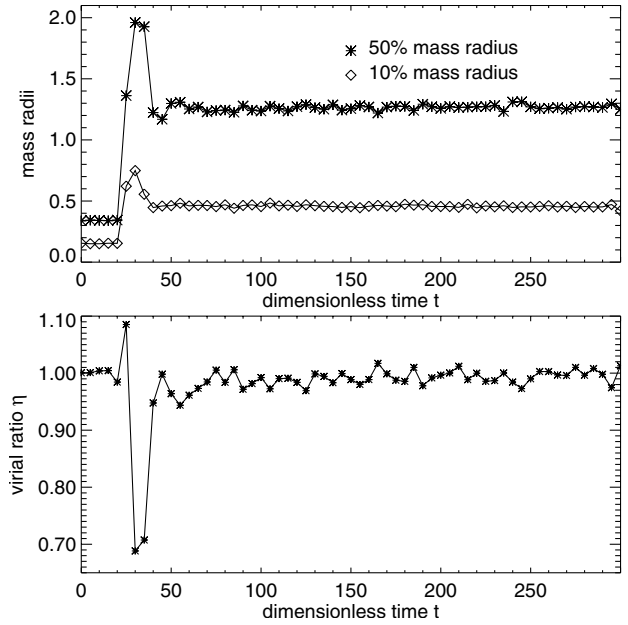


**Figure 2.** Time evolution of the mass radii (upper panel) and the virial ratio $\eta$ (lower panel) of the system shown in Fig. 1.

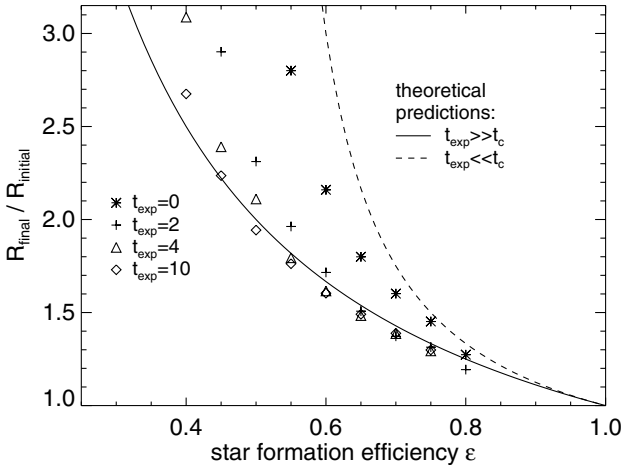


**Figure 3.** Ratio of the final to the initial half-mass radii versus SFE of the simulations (model N3) for various expulsion time-scales $t_{\rm exp}$.

cent for gas expulsion times $t_{\rm exp} = 0$, 2, 4 and 10, respectively. The Galactic average SFE in giant molecular clouds is of the order of a few per cent (Myers et al. 1986; Williams & McKee 1997). Koo (1999) has observed SFEs up to 15 per cent in the star-forming region W51B, maybe caused by shock-interaction with a spiral density wave. Given these SFEs, unrealistic high gas expulsion time-scales are required to obtain bound clusters. Only a few clouds show SFEs up to 30 per cent or 40 per cent (Lada 1992) and may stay bound.

## 3 COMBINED *N*-BODY AND HYDRODYNAMICAL SIMULATIONS

In Section 2, the effect of gas removal is treated as a time variable external potential. To describe the physics more properly, we extend our simulations using smoothed particle hydrodynamics [SPH, see Monaghan (1992) for a review]. We are using an SPH-code with variable smoothing length, individual particle time-steps (Bate, Bonnell & Price 1995) and collisionless *N*-body particles, which was made available by Matthew Bate.

The conversion from code units to physical units is the same as in Section 2.1. Additionally, we describe the internal energy of the gas with a dimensionless temperature that scales with $\hat{T} = G\hat{M}\,\mu\hat{R}^{-1}R_{\rm gas}^{-1}\gamma^{-1}$, where $\mu$ is the mean molecular weight, $R_{\rm gas}$ is the gas constant and $\gamma = 1/(\beta - 1)$, using the constant adiabatic exponent $\beta$. For an ideal gas with $\gamma = \frac{3}{2}$ and $\mu = 1.0$, we have $\hat{T} = 3.5 \times 10^3$ K.

### 3.1 Initial configuration and models for gas expulsion

Murray & Lin (1992) proposed as initial conditions pressure-confined protocluster clouds. As a reasonable initial configuration we therefore adopt a pressure-confined, isothermal Bonnor–Ebert (BE) sphere (Ebert 1955; Bonnor 1956), see Table 2.

Stars and star clusters form in molecular clouds with temperatures of the order of 10 K, and are stabilized by a turbulent velocity field. In this first approach we neglect turbulence. In order to prevent global collapse we then have to increase the temperature to its virial value $T = 2.7 \times 10^3$ K. This implies an energy $E_{\rm t} = \gamma M_{\rm c} R_{\rm gas} T/\mu$, corresponding to a turbulent velocity field with $v_{\rm tur} = \sqrt{2\,E_{\rm t}/M_{\rm c}} = 8.1\,{\rm km\,s^{-1}}$. Simulations of a cold (10 K) molecular gas cloud stabilized initially by a turbulent velocity field will be discussed in a subsequent paper.

To obtain a combined system of gas and stars, we add *N*-body particles with an equal density distribution, scaling the masses of the stars and the gas according to the SFE $\epsilon$. The velocity dispersion of the particles is chosen according to the temperature of the gas.

Isothermal spheres extend to infinity. In order to obtain a finite configuration, the gas density is set to zero at an arbitrary radius. To stabilize the gas sphere an external pressure is applied. This is not possible for particle systems. Therefore, the velocity dispersion of the *N*-body particles is decreased and the system is allowed to relax until a stable configuration is obtained.

Fig. 5 shows the evolution of one typical setup prior to gas removal. About 2 per cent of the *N*-body particles are lost, but after some oscillations the main part achieves an equilibrium state. This configuration is then used as initial model for following investigations.

The different models used are shown in Table 2.

To completely expel the residual gas from the cluster, the amount of energy fed into the gas must be comparable or greater than the binding energy of the gas, which in case of a homogeneous density distribution for gas and stars is

$$W_{\rm gas} = 4\pi\int_0^R \left(\tfrac{1}{2}\rho_{\rm g}\phi_{\rm g} + \rho_{\rm g}\phi_{\rm s}\right) r^2\,{\rm d}r = \frac{3(\epsilon^2 - 1)GM_{\rm c}^2}{5R}, \qquad (4)$$

where $\rho_{\rm g}$ and $\phi_{\rm g}$ are the constant density and the gravitational potential of the gas and $\phi_{\rm s}$ is the potential of the stars.

As the processes of gas expulsion are not well understood, we choose two simplified scenarios. In our first model we heat up the whole gas cloud by a factor of 10. As a result, the gas starts to expand and is removed. Our models are scale-free and can be applied to various initial conditions. For a typical molecular cloud with the parameters given in Section 2, the binding energy of the gas is $W_{\rm gas} \approx (\epsilon^2 - 1)\ 5.2 \times 10^{49}$ erg and the temperature increase is $\Delta T = 2.4 \times 10^4$ K, which is equivalent to an energy input of

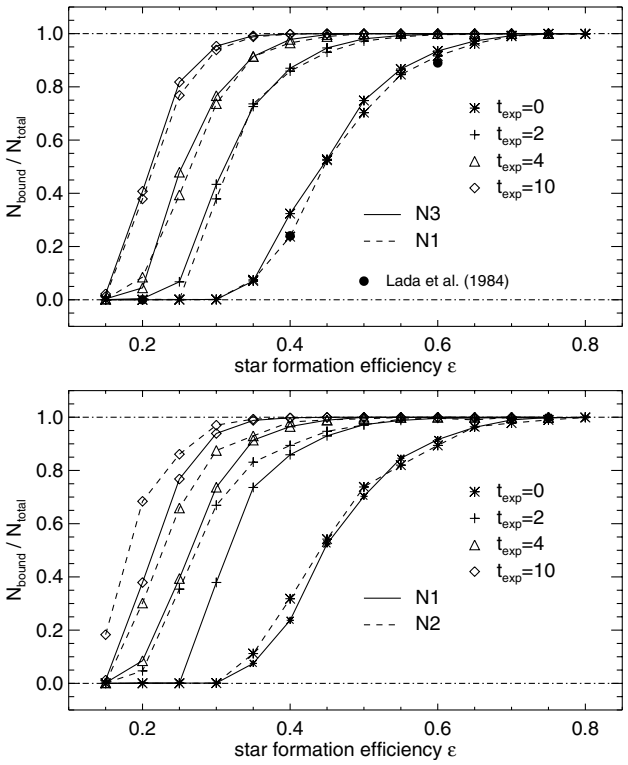


**Figure 4.** Ratio of the number of bound stars to the initial number of stars in the relaxed system after gas expulsion. Upper panel: models N1 and N3; lower panel: models N1 and N2; each symbol represents one run with given SFE and gas expulsion time; large dots are results taken from Lada et al. (1984), fig. 2 therein.

**Table 2.** Parameters of the initial configurations including gas dynamics (*N*-body and SPH). $r_h$, half-mass radius; $t_c$, crossing time at half-mass radius; $N$, number of particles; $T$, gas temperature; $\delta$, numerical (Plummer) smoothing length (*N*-body part only); $R$, cut-off radius; $\xi_b$, dimensionless cut-off radius, see Bonnor (1956); total mass (stars and gas) of all models was set to 1; all quantities are given in dimensionless code units (see text).

| Model | $r_h$ | $t_c$ | $N$ | $T$ | $\delta$ | $R$ | $\xi_b$ |
|---|---|---|---|---|---|---|---|
| S1 | 0.7 | 0.8 | 2×4000 | 0.76 | 0.01 | 1.0 | 4.0 |
| S2 | 0.7 | 0.8 | 2×11 045 | 0.76 | 0.05 | 1.0 | 4.0 |

$\Delta E = \gamma M_g R_{gas} \Delta T/\mu \approx (1-\epsilon)\ 5.9\times10^{50}$ erg, where $M_g = (1-\epsilon)M_c$ is the mass of the residual gas.

Can the ionizing radiation of massive OB stars be responsible for this kind of gas expulsion? A typical ionizing star has an initial Strömgren radius $R_{str} = 20n^{-2/3}\,\mathrm{pc\,cm^{-2}} = (1-\epsilon)^{-2/3}0.36\,\mathrm{pc}$ with the column density $n = \rho_g/(\mu m_p)$ of the surrounding gas, proton mass $m_p$ and $\mu = 2.36$ in the case of a molecular cloud. The mass therein is $M_{str} = 4\pi/3\rho_g R_{str}^3 = (1-\epsilon)^{-1}4.7\,M_\odot$ (Franco, Shore & Tenorio-Tagle 1994). The time-dependent mass inside the expanding H II region is (Franco et al. 1994)

$$M_i = M_{str}\left(1+\frac{7a_i t}{4R_{str}}\right)^{6/7}, \qquad (5)$$

where $a_i = \sqrt{R_{gas}T/\mu} = 8.0\,\mathrm{km\,s^{-1}}$ is the speed of sound inside the ionized region with $T = 1.0\times10^4$ K and $\mu = 1.3$. After $t = 10^7$ yr, the typical lifetime of an OB star, we have $M_i \approx (1-\epsilon)^{-3/7}7.9\times10^2\,M_\odot$. To completely ionize the whole gas cloud, we therefore need $M_g/M_i = (1-\epsilon)^{10/7}1.3\times10^2$ OB stars. This is in good agreement with reasonable initial mass functions. Knödlseder (2000) showed that Cygnus OB2, a probable young GC in the Galactic disc, contains about 120 O stars, while the total mass could be as high as $10^5\,M_\odot$. We conclude, that the ionizing radiation from high-mass stars is sufficient to expel the residual gas.

In our second scenario we simulate an outward propagating shock front, disrupting the gas cloud. Such shock fronts may be generated by combined supernova explosions and winds from central high-mass stars. The formation of supershells and their ability to disrupt the cloud are discussed in various papers with regard to chemical self-enrichment of GCs (Morgan & Lake 1989; Brown, Burkert & Truran1995; Parmentier et al. 1999). Goodwin, Pearce & Thomas (2001) investigate single supernovae in gas clouds. In our simulation we heat up a small inner core with radius $R = 0.2$. All 229 SPH particles inside are heated by a factor of 200. Applying again the typical parameters given in Section 2, the temperature increase is $\Delta T = 5.2\times10^5$ K, corresponding to an energy input of $\Delta E \approx (1-\epsilon)\ 2.7\times10^{50}$ erg. This is less than the typical energy $E_{SN} = 10^{51}$ erg of a single supernova. However, it must be taken into account that only a few per cent of the supernova energy is fed into the gas (Goodwin et al. 2001) and therefore several supernovae may be needed to disrupt the cloud.

### 3.2 Evolution of the cluster during and after gas expulsion

Fig. 6 shows the time evolution of a system with gas ejection in a supershell. The shell reaches a velocity up to 5 times the speed of sound of the initial system. Once the internal pressure of the expanding gas is smaller than the adopted external pressure, the outward propagating shell becomes unstable and develops substructures. At that stage, less than two crossing times after the gas removal started, the gas density in the cluster region is so low that its gravitational effect on the stellar component is negligible. We therefore remove the gas and follow the evolution of the stars alone. The globally heated cloud models show a very similar evolution and are treated in the same manner.

Fig. 7 corresponds to Fig. 4 in the pure *N*-body case. For comparison, the broken curves reproduce the results of the pure *N*-body simulations.

For instantaneous gas expulsion (all the gas particles are removed at once), corresponding to the case $t_{exp} = 0$ in Section 2, the simulations using the BE sphere as initial configuration are in very good agreement with the simulations using a King density distribution. The slightly higher crossing times of the BE sphere (see Table 2) may cause the small differences for small SFEs: the simulation was not run long enough for all particles to become unbound. We therefore conclude that the density distribution has no influence on the number of bound particles after gas expulsion, at least if $t_{exp} = 0$.

The crosses in Fig. 7, lower panel, show system S1 where the temperature of the whole cloud was increased by a factor of 10 with respect to the equilibrium model. The number of bound stars increases slightly compared with the case with instantaneous gas expulsion. The diamonds in the upper panel show the results for a cloud centrally heated to $T = 152$ (system S2). Compared with the first model S1, no significant differences are visible. Again, the number of bound stars increases slightly. However, the gas

expulsion process in both cases is much faster than the time-scales adopted in Section 2. Therefore, also in more realistic cases, high SFEs are needed to sustain a bound star cluster.

One way out may be a collapse of the star cluster before the gas is completely expelled, leading to a higher 'effective SFE'. Lada et al. (1984) and Verschueren (1990) proposed a low or zero initial velocity dispersion to explain the collapse. Saiyadpour, Deiss & Kegel (1997) considered the effect of dynamical friction on the stellar cluster.

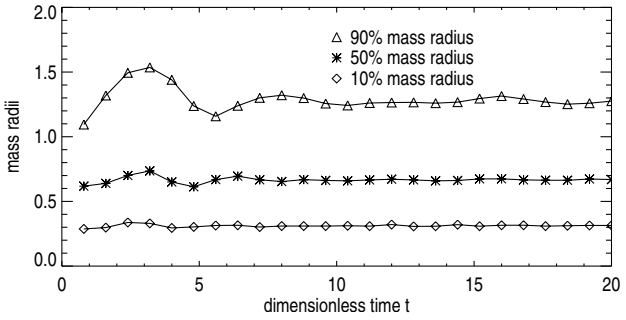


**Figure 5.** Evolution of the mass radii of a combined *N*-body and SPH simulation. At the end of the stability test the system is in equilibrium.

We implement the first approach by setting the initial velocity dispersion of the stars to zero and heating the whole gas cloud. In each of the simulations, the cluster virializes after gas expulsion within a half-mass radius that is about 40 per cent of the initial radius, or about 2.7 pc applying again the typical units. Only the few stars that gain velocities higher than the escape velocity of the cluster are ejected. For a wide SFE range the percentage of bound stars at the end of the simulations is nearly constant and higher than 80 per cent (Fig. 7, upper panel, triangles). Even our run with the lowest SFE $\epsilon = 0.02$ leads to a bound system. However, small SFEs by definition lead to low-mass star clusters. In order to obtain observed GC masses, our initial cloud mass has to be rescaled to higher values. Even if this scenario is very unlikely, for reasonable initial conditions bound clusters can be formed with masses and radii similar to observed GCs.

## 4 CONCLUSIONS AND OUTLOOK

*N*-body and combined *N*-body and SPH calculations to investigate the influence of the residual gas expulsion on the stellar part in star-forming regions are presented.

We show that in the case of instantaneous gas expulsion, clusters with SFEs greater than $\epsilon = 0.45$ can keep more than 50 per cent of the initial stars. Clusters with SFEs less than $\epsilon = 0.40$

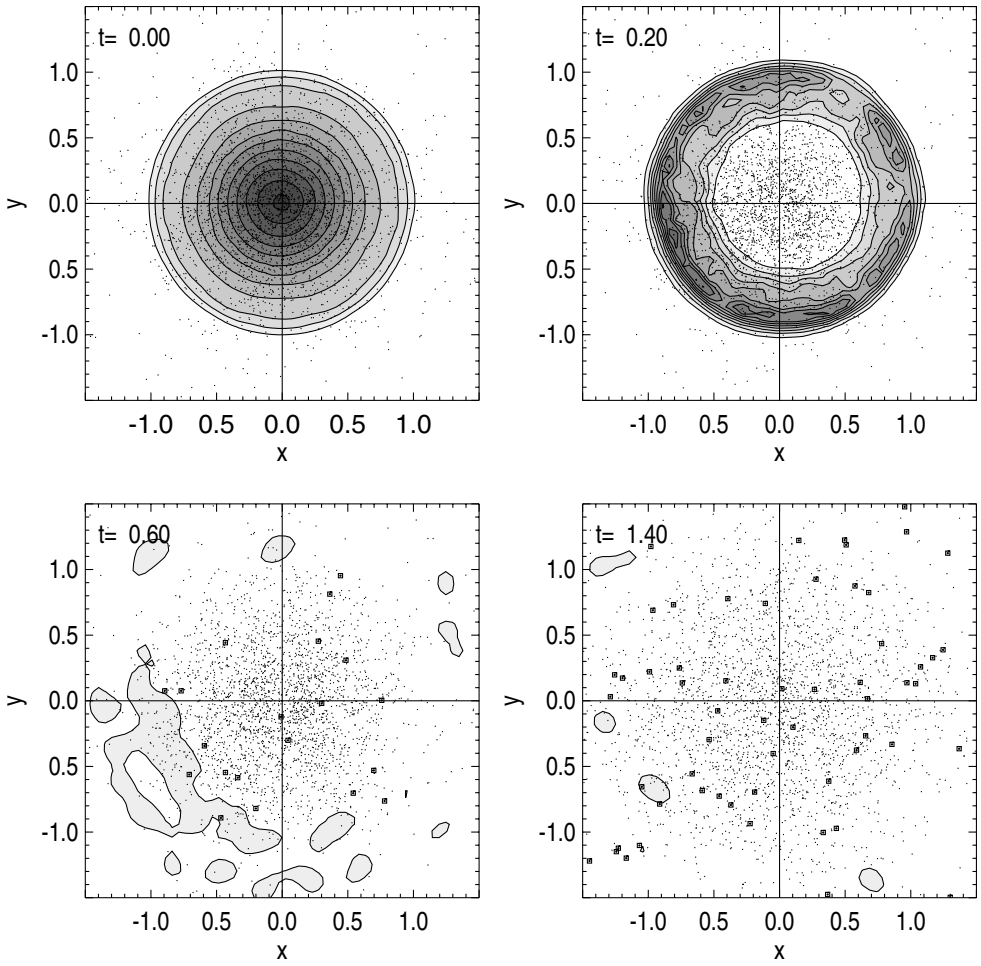


**Figure 6.** Time evolution of model S2 during the gas expulsion phase (dimensionless time *t*). The SFE is $\epsilon = 0.4$ and central heating is applied. The plots show the *N*-body particles (small dots) projected on to the *x*–*y*-plane (only every fourth particle is shown); unbound particles are indicated by squares. The contour lines indicate the gas density in the *x*–*y*-plane in steps of 0.025.

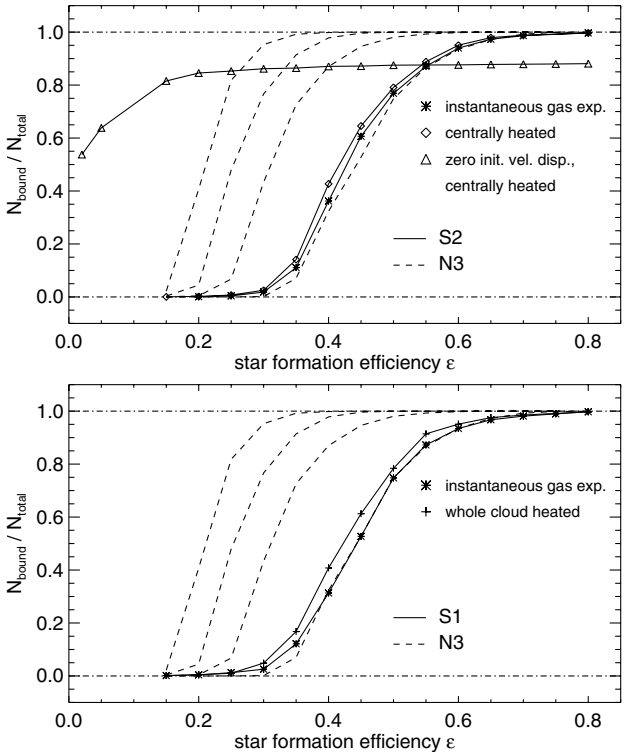


**Figure 7.** Ratio of the number of bound stars to the initial number of stars in the relaxed system after gas expulsion; broken curves indicate the results from Fig. 4, model N3.

are dissolved. Different concentrations of the initial models show no effect at all on the number of bound stars if the gas is expelled instantaneously.

We confirm that gas expulsion time-scales which are several times longer than the crossing time of the cluster can decrease the SFE needed to sustain bound clusters considerably.

However, our simulations including the proper dynamics of the residual gas show that in order to destroy the whole cloud by global heating or by supershells the gas expulsion must take place on a short time-scale, requiring a high SFE. Only a few star-forming regions show such high SFEs. However, if the global SFE averaged over a molecular cloud is low, bound clusters can form in regions where the local SFE is high (Adams 2000).

Another possibility to form bound clusters with small efficiencies is indicated from the recent simulations of Klessen & Burkert (2000, 2001), who study star formation in turbulent molecular clouds. They find that the stars form preferentially in fragmenting filaments, where most of the turbulent energy is dissipated. The newly formed protostars have small relative velocities corresponding to virial ratios $\eta = -2E_{\rm kin}/E_{\rm pot} < 1$. We demonstrate that models with stars having an initial zero velocity dispersion lead to a compaction of the cluster and can explain bound systems even in low SFE regions. For SFEs as low as $\epsilon = 0.15$ more than 80 per cent of the stars stay bound. Bound systems are obtained even with SFEs lower than 10 per cent. For future investigations it is essential to know the velocity dispersion of newly born stars in clusters.

## ACKNOWLEDGMENTS

We would like to thank Matthew Bate for making available his combined *N*-body and SPH code. Also thanks to Pavel Kroupa for his very useful comments and to Charles J. Lada for his valuable suggestions as referee for this paper.

## REFERENCES

Adams F. C., 2000, ApJ, 542, 964
Barnes J., Hut P., 1986, Nat, 324, 446
Bate M. R., Bonnell I. A., Price N. M., 1995, MNRAS, 277, 362
Binney J., Tremaine S., 1987, Galactic Dynamics. Princeton Univ. Press, Princeton, NJ
Bonnor W. B., 1956, MNRAS, 116, 351
Brown J. H., Burkert A., Truran J. W., 1995, ApJ, 440, 666
Ebert R., 1955, Z. Astrophys., 37, 217
Franco J., Shore S. N., Tenorio–Tagle G., 1994, ApJ, 436, 795
Goodwin S. P., 1997, MNRAS, 284, 785
Goodwin S. P., Pearce F. R., Thomas P. A., 2001, ApJ, submitted (astro-ph/0001180),
Hills J. G., 1980, ApJ, 225, 986
King I. R., 1966, AJ, 71, 64
Klessen R. S., Burkert A., 2000, ApJS, 128, 287
Klessen R. S., Burkert A., 2001, ApJ, 549, 386
Knödlseder J., 2000, A&A, 360, 539
Koo B.-C., 1999, ApJ, 518, 760
Lada C. J., Margulis M., Dearborn D., 1984, ApJ, 285, 141
Lada E. A., 1992, ApJ, 393, L25
Mathieu R. D., 1983, ApJ, 267, L97
Monaghan J. J., 1992, ARAA, 30, 543
Morgan S., Lake G., 1989, ApJ, 339, 271
Murray S. D., Lin D. N. C., 1992, ApJ, 400, 265
Myers P. C., Dame T. M., Thaddeus P., Cohen R. S., Silverberg R. F., Dwek E., Hauser M. G., 1986, ApJ, 301, 398
Parmentier G., Jehin E., Magain P., Neuforge C., Noels A., Thoul A. A., 1999, A&A, 352, 138
Saiyadpour A., Deiss B. M., Kegel W. H., 1997, A&A, 322, 756
Verschueren W., 1990, A&A, 234, 156
Williams J. P., McKee C. F., 1997, ApJ, 476, 166

This paper has been typeset from a TEX/LATEX file prepared by the author.